

# RSC Advances



This is an *Accepted Manuscript*, which has been through the Royal Society of Chemistry peer review process and has been accepted for publication.

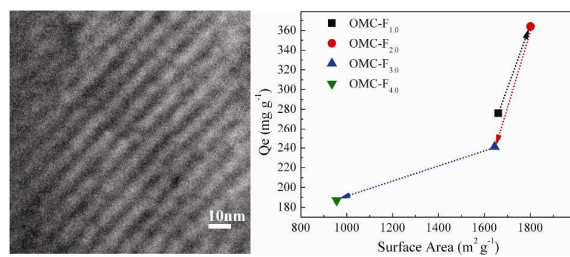
*Accepted Manuscripts* are published online shortly after acceptance, before technical editing, formatting and proof reading. Using this free service, authors can make their results available to the community, in citable form, before we publish the edited article. This *Accepted Manuscript* will be replaced by the edited, formatted and paginated article as soon as this is available.

You can find more information about *Accepted Manuscripts* in the [Information for Authors](#).

Please note that technical editing may introduce minor changes to the text and/or graphics, which may alter content. The journal's standard [Terms & Conditions](#) and the [Ethical guidelines](#) still apply. In no event shall the Royal Society of Chemistry be held responsible for any errors or omissions in this *Accepted Manuscript* or any consequences arising from the use of any information it contains.

## Graphical Abstract

High Surface area ordered mesoporous carbons were fabricated as superior adsorbents for ultrahigh decontamination of di(2-ethylhexyl)phthalate from model water pollutant.



# Tuned surface area and mesopore diameter of ordered mesoporous carbon: ultrahigh decontamination of di(2-ethylhexyl)phthalate

Pranav K. Tripathi, Mingxian Liu\* and Lihua Gan\*

Department of Chemistry, Tongji University, 1239 Siping Road, Shanghai 200092, China

**Abstract:** Synthesis of carbon materials with enhanced surface area, regular and tuned pore diameter are always being the great challenges. In this report, ordered mesoporous carbons (OMCs) were synthesized by the one-step assembly of tri-constituents, and the OMCs were applied as an adsorbent for the removal of highly hazardous water pollutant: di(2-ethylhexyl)phthalate (DEHP). Phloroglucinol-formaldehyde based carbon precursor was in-situ prepared in the assembly of tri-constituents and the surface area and mesopore diameter of OMCs were tuned by the variation of molar ratio of formaldehyde to phloroglucinol. Small angle X-ray diffraction patterns revealed that the obtained carbons are highly ordered, which is in agreement with the measuring results of transmission electron microscopy at low and high resolution. Scanning electron microscopy images demonstrate that OMC-F<sub>2.0</sub> has hierarchical morphology. Nitrogen adsorption-desorption measurements revealed that the surface area of OMCs (956-1801 m<sup>2</sup> g<sup>-1</sup>) were depend on molar ratio of the carbon precursor constituent (formaldehyde to phloroglucinol). By the variation of molar ratio of formaldehyde to

---

\*Corresponding author: Tel.: +86 21 65982654-8430, Fax: +86 21 65981097.

E-mail address: [liumx@tongji.edu.cn](mailto:liumx@tongji.edu.cn) (M. Liu), [ganlh@tongji.edu.cn](mailto:ganlh@tongji.edu.cn) (L. Gan)

phloroglucinol from 1.0 to 4.0, the mesopore diameter of OMCs was shifted to higher side from 2.1 to 3.1 nm. DEHP was efficiently removed from the model water pollutant by OMCs. The OMC-F<sub>2.0</sub> has achieved highest adsorption capacity of 364 mg g<sup>-1</sup> for the removal of DEHP. The adsorption equilibrium data were treated with two mathematical models of Langmuir and Freundlich, and the results revealed that decontamination was more favorable with Langmuir model. It concludes that removal of DEHP by OMCs depends on the surface area and DEHP molecules occupied the porous space of OMCs in monolayer manner.

## 1. Introduction

Water is essential for survival of life; on the contrary it became the major sources of diseases because water stream is exponentially contaminating.<sup>1</sup> Increasing human dependency on plastic materials bloomed the use of di(2-ethylhexyl)phthalate (DEHP) as preferred plasticizer. DEHP is one of the highly health threat water contaminate to living beings even at the very low concentration and considered as endocrine disruptive chemical.<sup>2</sup> The prolong contact of DEHP contaminated water can lead to damage of reproductive capability, short of memory and many others diseases.<sup>3</sup> International agency for research on cancer considered DEHP as possibly carcinogenic agent to humans (Group 2B).<sup>4</sup> Sources of water contamination by DEHP are discharge wastewater from manufacturing unit of DEHP, tubes, tires, soft plastics, and leaching from landfill site of plastic materials. DEHP is increasingly detecting in water bodies.<sup>3, 5, 6</sup> DEHP has a persistent nature, thus conventional treatment methods are not feasible for the removal of DEHP from contaminated water and wastewater.<sup>7, 8</sup> Therefore it is very important to remove DEHP from polluted water and wastewater by effective treatment technology.

Adsorption is one of the potential method for the removal of soluble and insoluble water pollutants.<sup>1, 9</sup> Activated carbon (AC) is widely used as an adsorbent for water and wastewater

treatment because of high surface area and chemically inert nature. However, AC has small and irregular micropores (<2 nm) which dramatically limit the capability for the removal of large size molecules such as DEHP (**Table 1**). Several studies revealed that abundant micropores of AC limit the access of large internal porous area to the big size molecules.<sup>10-12</sup> In this regards adsorbents development with large and regular pore diameter have been evoked the great interest. Ordered mesoporous carbons (OMCs) have been extensively investigated as modern porous materials and considered as promising adsorbents due to their high surface area, large pore volume and uniform pore diameter.<sup>13</sup> These features of OMCs offer the free movements of atoms, ions and molecules throughout the material and allow to occupy the large available internal area.<sup>9, 14</sup>

In regards to the adsorption, surface area is always been the main attraction.<sup>1, 15</sup> Under above consideration several techniques have been applied via soft template approach to tune the surface area of OMCs.<sup>11, 16</sup> Generally, soft template based method is two step assembly process of the constituents, and it has multistep processing flaws like hard template.<sup>17</sup> For example, Zhao group has always used the pre-polymerized carbon precursor ‘resol’ in tri-constituent system<sup>16, 18-21</sup> and many other groups whoever used resol as carbon precursor.<sup>22, 23</sup> Dai and Yuan groups have made the approach to find a single step synthesis process of OMCs but fail to tune the surface area.<sup>24, 25</sup> Herein we attempted one-step approach to assemble the tri-constituents via evaporation induced self assembly (EISA) for the tuning of surface area and pore diameter of OMCs. In one-step assembly of tri-constituents, the carbon precursor of phloroglucinol-formaldehyde was in-situ prepared during the assembly of tri-block copolymer, inorganic precursor and carbon precursor. The surface area and pore diameter of OMCs were tuned by the molar ratio variation of formaldehyde to phloroglucinol. The resultant OMCs were used as environmental adsorbents for

the removal of DEHP from water. The molecular distribution of DEHP in the pore channels of OMCs was studied by the use of two mathematical models, i.e., Langmuir and Freundlich.

## 2. Experimental

### 2.1. Chemicals

Pluronic F127 ( $M_w=12600$ ,  $PEO_{106}PPO_{70}PEO_{106}$ ) was purchased from Aldrich. Tetraethyl orthosilicate (TEOS), phloroglucinol were purchased from Aladdin. Formaldehyde, ethanol, hydrochloric acid and DEHP were purchased from Sinopharm Chemical Co., Ltd. All chemicals were used as received without any further purification.

### 2.2. Synthesis of OMCs

Evaporation induced self assembly (EISA) method was applied to assemble the tri-constituents in one-step process. Structure directing agent Pluronic F127 (1.6 g) was dissolved in acidic ethanol solution which was prepared by using 20.0 g ethanol and 1.0 g hydrochloric acid of 0.1 M. Followed by addition of 2.0 g inorganic precursor tetraethyl orthosilicate (TEOS). Further, 4 mmol phloroglucinol and 1-4 mmol formaldehyde were added and stirred for 60 min at room temperature. All three constituents were assembled in the one-step process. After 60 min stirring, the assembled mixture was transferred into dish and placed at room temperature for ~5 h to evaporate ethanol. After the evaporation of ethanol, thermal polymerization was conducted at 100°C for 24 h in an electric oven, thin layer membrane was obtained. The membrane was scratched from the dish and was carbonized in the  $N_2$  flow tubular furnace at 350°C for 3 h and 800°C for 8 h with the following temperature program: 1°C  $min^{-1}$  below 600°C and 5°C  $min^{-1}$  above 600°C.<sup>26</sup> After carbonization, natural cooling process was performed. The resultant

carbon-silica composites were immersed in 10% HF solution for 24 h to etch the silica, followed by water washing until neutral pH reached; the obtained wet carbon was placed in oven at 100°C for the overnight drying. The resultant carbon was denoted as OMC-F<sub>x</sub>, where x stands the molar ratio of formaldehyde to phloroglucinol.

### 2.3. Characterization

Nitrogen adsorption and desorption isotherms were measured at -196°C using Micromeritics Tristar 3000 gas adsorption analyzer. Before measurement, the samples were degassed in vacuum at 200°C for at least 4 h. Brunauer-Emmett-Teller (BET) method was utilized to calculate the specific surface areas ( $S_{\text{BET}}$ ) by using adsorption data in a relative pressure range from 0.05 to 0.25. Mesopore diameter and total pore volumes ( $V_{\text{t}}$ ) were calculated by Barret-Joyner-Halenda (BJH) model and micropore volumes ( $V_{\text{mic}}$ ) were calculated from the t-plot. Powder small angle X-ray diffraction (SAXRD) was carried out by using X-ray diffractometer (Bruker AXS, D8 Advance). The structural morphologies of the resultant OMCs were observed by using transmission electron microscope (TEM, JEM-2100) and scanning electron microscope (SEM, Hitachi, S-4800).

### 2.4. Adsorption Studies

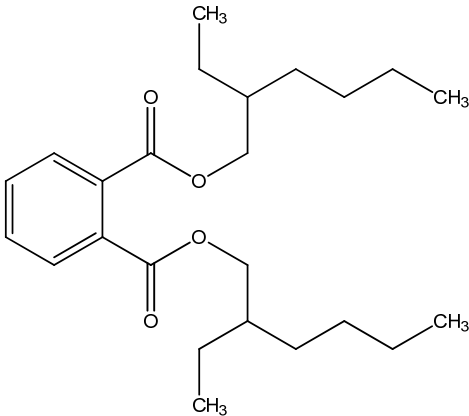
The batch adsorption experiments of OMCs were performed using DEHP (Chemical structure and physical properties of DEHP was shown in **Table 1**) as a water pollutant. Since DEHP is poorly dissolved in water, therefore, the stock solution of DEHP was prepared by dissolving 1.0 g DEHP in 1000 mL ethanol. Further different concentration of water soluble model pollutant of DEHP was prepared from 20 to 285 mg L<sup>-1</sup> by dissolving the stock solution in distilled water. Adsorption capacities of OMCs were measured by varying the initial DEHP

concentration. In a typical experiment, 0.010 g adsorbent was contacted with 25 mL of aqueous solution with different concentration of DEHP (20 to 285 mg L<sup>-1</sup>). The mixture of pollutant and adsorbent was agitated with 150±5 rpm until the equilibrium is reached at temperature 25±0.1°C. Prior to analysis, the suspension was separated using a 0.45 µm membrane filter. The concentration of DEHP solution was determined using a calibration curve obtained using high-performance liquid chromatography (HPLC, Agilent 1260 Infinity) system with a Agilent ZORBAX SB-C18, 5 µm, 4.6\*250 mm column and a UV absorbance detector (G1314B) operated at 235 nm. The flow of mobile phase was 1.0 mL min<sup>-1</sup> of 90% acetonitrile and 10% methanol (HPLC grade). The amount of adsorbed DEHP,  $Q_e$  (mg g<sup>-1</sup>), was calculated by

$$Q_e = \frac{(C_0 - C_e)V}{W} \quad (1)$$

where  $C_0$  and  $C_e$  are the initial and equilibrium concentration (mg L<sup>-1</sup>), respectively;  $V$  is the volume of DEHP aqueous solution (L), and  $W$  is the weight (g) of OMCs adsorbent.

**Table 1** Chemical structure and physical properties of DEHP

Pollutant IUPAC Name	Chemical Structure	Molecular weight (g mol <sup>-1</sup> )	Molecular width (nm)	Molecular length (nm)	Ref.
DEHP		390.56	0.525	1.658	<a href="#">27</a>

### 3. Results and Discussion



### 3.1. Synthesis of OMCs

OMCs were synthesized by the one-step self assembly of tri-constituents via EISA method. As it is shown in **Fig. 1**, the structure directing agent (Pluronic F127), organic precursor (phloroglucinol-formaldehyde) and inorganic precursor (TEOS) are self assembled via hydrogen bonding in acidic ethanol solution. Formaldehyde acted as bridging agent between two phloroglucinol via electrophilic substitution and elimination of H<sub>2</sub>O.<sup>28</sup> In the competitive cooperative self-assembly of organic-organic (phloroglucinol-formaldehyde-Pluronic F127) and organic-inorganic (phloroglucinol-formaldehyde-TEOS and Pluronic F127-TEOS), the hydrogen bonding played a vital role. On the one hand, phloroglucinol has three meta hydroxyl groups (positions 1, 3, 5) which are considered as sanative towards the hydrogen bonding.<sup>26</sup> On the other hand, Pluronic F127 has long PEO domain which could allow forming the organic-organic self assembly via enhanced hydrogen bonding (as shown in **Fig. 1**)<sup>24</sup>, and it favour the organization of ordered nanocomposite mesostructures.<sup>16</sup> In the self assembly process, the PPO domain of Pluronic F127 forms the core of assembled constituents.<sup>29</sup> The evaporation of ethanol and thermal polymerization were able to form 3D hexagonal array of all three assembled constituents.<sup>16</sup> The carbon precursor of phloroglucinol-formaldehyde was in-situ prepared, instead the use of pre-polymerized carbon precursor. The molar ratio variation of formaldehyde to phloroglucinol was able to tuning the surface area of OMCs. Carbon-silica composite was obtained after the carbonization of assembled hexagonal polymeric array of tri-constituents at higher temperature in nitrogen flow atmosphere. Inorganic precursor (TEOS) was used to prevent the shrinkage during the carbonization process<sup>16</sup> and also for the generation of micropores in the mesopore wall of OMCs after the etching of silica from carbon-silica

composites. The etching of silica from carbon-silica composite was able to develop the attractive textural featured OMCs.

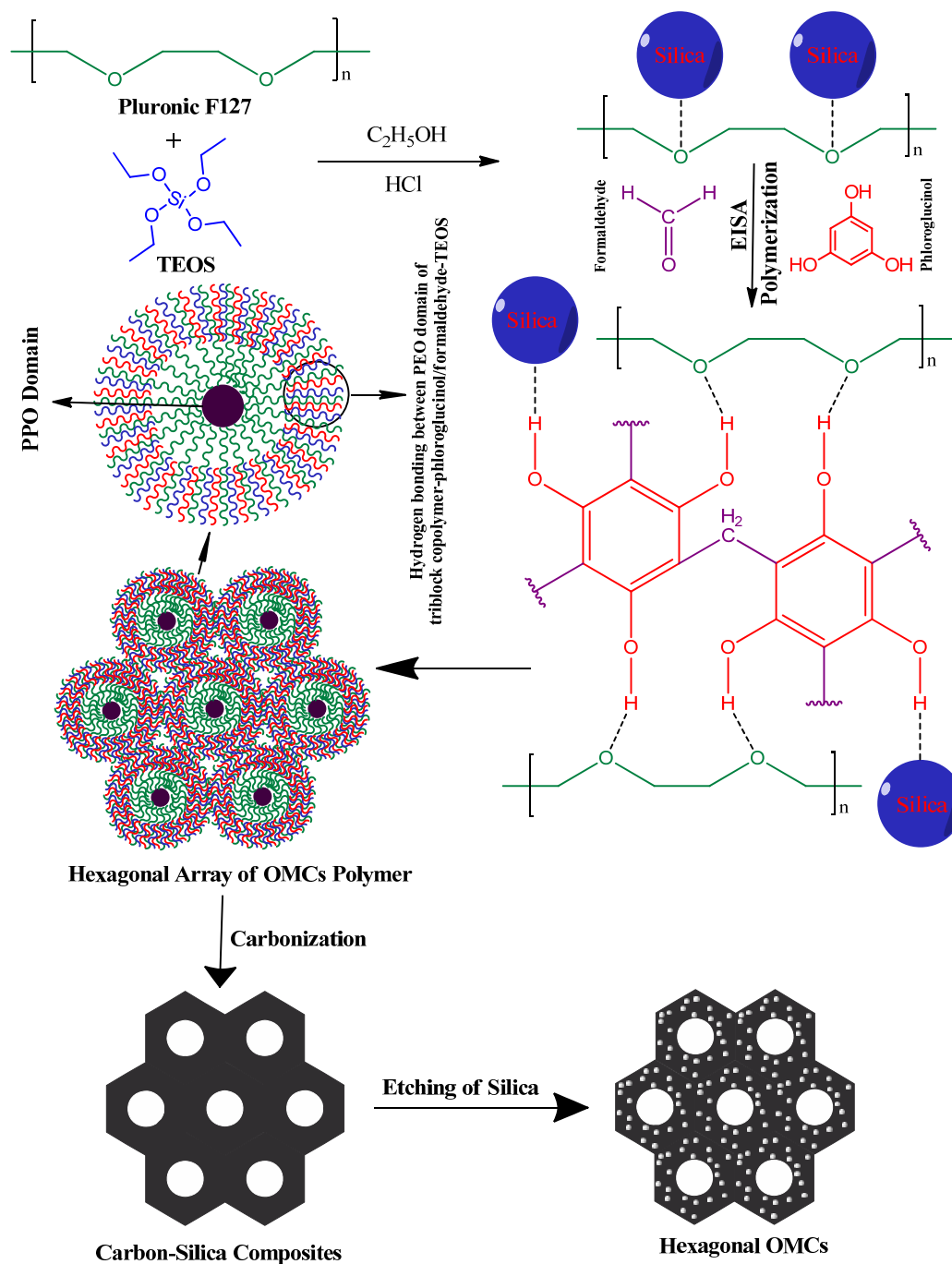


**Fig. 1** Schematic representation of OMC- $F_x$  synthesis.

### 3.2. Evaluation of surface area, pore diameter and pore volume of OMCs

The surface area, pore volume and pore diameter of OMCs were evaluated by nitrogen adsorption-desorption analysis. The N<sub>2</sub> adsorption-desorption isotherms of OMCs are presented in **Fig. 2a**. All OMCs are assigned to type IV with H1 hysteresis loop according to international union of pure and applied chemistry (IUPAC) classification.<sup>30, 31</sup> Type IV curve and H1 hysteresis indicating the presence of high level and uniform mesoporosity in OMCs.<sup>30</sup> The steep increase at low relative pressure region ( $p/p_0$ ) of 0.008-0.025 could be related to the nitrogen molecular adsorption in the micropores of OMCs. This initial process has been related with the monolayer adsorption on each micropore wall, therefore a single layer or double layers can be formed between two walls.<sup>32</sup> On the other hand, well define H1 loop at high relative pressure region ( $P/P_0$  0.5 to 0.85) is attributed to condensation in mesopores of OMCs. All hysteresis fits to H1 with little difference, for example, OMC-F<sub>2.0</sub> has parallel steep of adsorption-desorption isotherms which could be assigned to uniform mesopore diameter throughout the materials. The uniformity of pore diameter of OMC-F<sub>2.0</sub> can be seen in pore size distribution curve of **Fig. 2b**. By the gradual increment of the molar ratio of formaldehyde to phloroglucinol, hysteresis shifted to higher relative pressure side which could attribute to pore size increment and the pore size distribution curve was in agreement with hysteresis shift towards higher side of **Fig. 2b**. The pore diameter was increased from 2.1 to 3.1, as shown in **Table 2**. While upto 2.0 molar ratio, there was no major increment noticed. In our previous study, microporosity were enormously depended on the removal of silica from the carbon-silica composite of ordered carbon derived from tri-constituents assembly.<sup>13</sup> In this work, silica also played the similar role, and its removal from the carbon-silica composites after the carbonization of assembled tri-constituents results in high microporosity of OMCs. The microporosity also affected by the molar ratio of

formaldehyde to phloroglucinol, as shown in **Table 2** and **Fig. 2b**. Beyond optimum molar ratio (2.0), micropore volume was decreased from 0.8 to 0.2 cm<sup>3</sup> g<sup>-1</sup>. It could be due to the collapse of open framework of formaldehyde-phloroglucinol at high ratio. On the other hand, no major increment in mesoporosity was observed. However, maximum total pore volume (2.1 cm<sup>3</sup> g<sup>-1</sup>) was observed in OMC-F<sub>3,0</sub>, it is little higher (0.1 cm<sup>3</sup> g<sup>-1</sup>) than that of OMC-F<sub>2,0</sub> prepared at the optimum molar ratio. Importantly, surface area was also depended on the molar ratio of formaldehyde to phloroglucinol in one-step assembly process of tri-constituents as other texture features. The surface area was calculated by using BET method at relative pressure P/P<sub>0</sub> from 0.07 to 0.20, and in this range all OMCs followed straight line and reported correlation coefficient was 1. As the molar ratio of formaldehyde to phloroglucinol was increased to higher value (form 1.0 to 2.0) uptake volume of N<sub>2</sub> was also increased (form 344 and 445 cm<sup>3</sup> g<sup>-1</sup> to 364 and 476 cm<sup>3</sup> g<sup>-1</sup>) which contributed to high surface area of OMCs. However, increasing the molar ratio of formaldehyde to phloroglucinol after optimum molar ratio of 2.0 was failed to enhance the surface area. It is mainly based on bulk porosity, and it was assumed that at optimum molar ratio of formaldehyde to phloroglucinol in one-step assembly process of tri-constituents made open and smaller size hydrocarbon networks which generated high porosity<sup>33</sup> and attributed to high surface area. Dai and Yuan used phloroglucinol-formaldehyde based precursor to synthesis the OMCs<sup>24, 25</sup> but in their work surface area was not very high to use as adsorbents. The above assumption is supported by the micropore area and external surface area, as shown in **Table 2**.

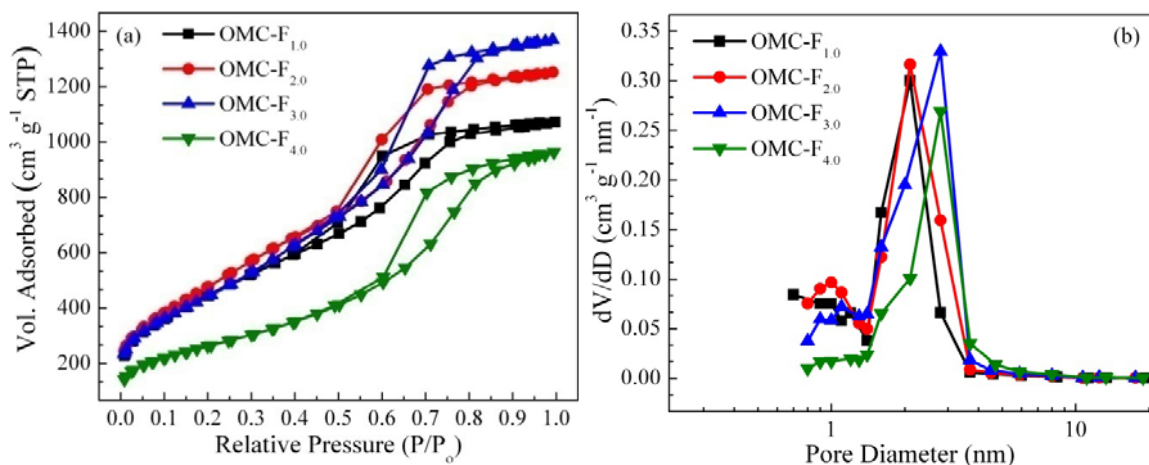


**Fig. 2** N<sub>2</sub> adsorption-desorption isotherm of OMC-F<sub>1.0-4.0</sub> (a) and corresponding pore size distribution curve (b).

**Table 2** Surface area, pore size/volume and adsorption capacities of OMCs

Adsorbent	$S_{\text{BET}}$ ( $\text{m}^2 \text{g}^{-1}$ )	Micropore Area ( $\text{m}^2$ $\text{g}^{-1}$ )	External Surface Area ( $\text{m}^2$ $\text{g}^{-1}$ )	$V_{\text{Total}}$ ( $\text{cm}^3$ $\text{g}^{-1}$ )	$V_{\text{meso}}$ ( $\text{cm}^3 \text{g}^{-1}$ )	$V_{\text{micro}}$ ( $\text{cm}^3 \text{g}^{-1}$ )	D (nm)	$Q_e$ ( $\text{mg g}^{-1}$ )
OMC-F <sub>1.0</sub>	1660	1101	559	1.7	0.9	0.8	2.1	276
OMC-F <sub>2.0</sub>	1801	1065	736	2.0	1.2	0.8	2.3	364
OMC-F <sub>3.0</sub>	1644	684	960	2.1	1.4	0.7	2.9	241
OMC-F <sub>4.0</sub>	956	110	846	1.5	1.3	0.2	3.1	187

### 3.3. Structure and morphology features of OMCs

SAXRD patterns of OMCs are presented in **Fig. 3**. All OMCs had one strong and one weak peak which can be indexed to (100) and (110) reflection, corresponding to 2D hexagonal ordered mesostructure with space group  $p6mm$  symmetry.<sup>34</sup> Effect of the molar ratio of formaldehyde to phloroglucinol was also seen in the order structure of OMCs. Increasing the molar ratio from 1.0 to 2.0, the (100) and (110) indexed peaks become narrow, suggesting that the ordered hexagonal mesostructure was retained and become better. Further increment of the molar ratio after an optimum molar ratio (2.0), (100) indexed peak was shifted to left side and visibility of (110)

indexed peak became poor. At the molar ratio of 4.0, (100) indexed peak became sharper and narrower and (110) indexed peak was very poorly appeared. It indicated the partial collapse of mesostructure regularity<sup>35</sup> and which might occurred due to such a high molar ratio of formaldehyde to phloroglucinol in one-step assembly process of tri-constituents.

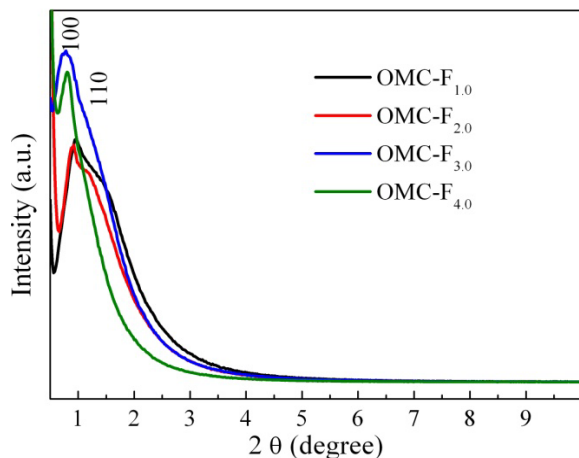


**Fig. 3** Small angle X-ray diffraction patterns of OMC-F<sub>1.0-4.0</sub>.

The surface morphology and order structure of OMC-F<sub>2.0</sub> are presented in **Fig. 4**. **Fig. 4a** reveals that large domain of OMC-F<sub>2.0</sub> has uniform mesopore channels. **Fig. 4b** reveals that some of the mesopores are collapsed with each other and formed wide mesopore; it could be attributed to the etching of silica from mesopore walls. It was noted that there was no changes observed in the structure due to etching of silica as it shown in **Fig. 3**. Furthermore, obtained mesopore diameter of OMC-F<sub>2.0</sub> from BJH method was also in the correlation with FESEM images (**Fig. 4b**). Order morphology of OMC-F<sub>2.0</sub> can be seen in TEM image (**Fig. 4c**). It reveals that large segments are ordered and it is in agreement with SAXRD patterns. The irregularity in ordered channel can be seen in HRTEM image (**Fig. 4d**), indicating the etching of silica from the wall of carbon-silica composites. It confirms that etching process was responsible for enhancing the surface area without failing to destroy the ordered morphology.

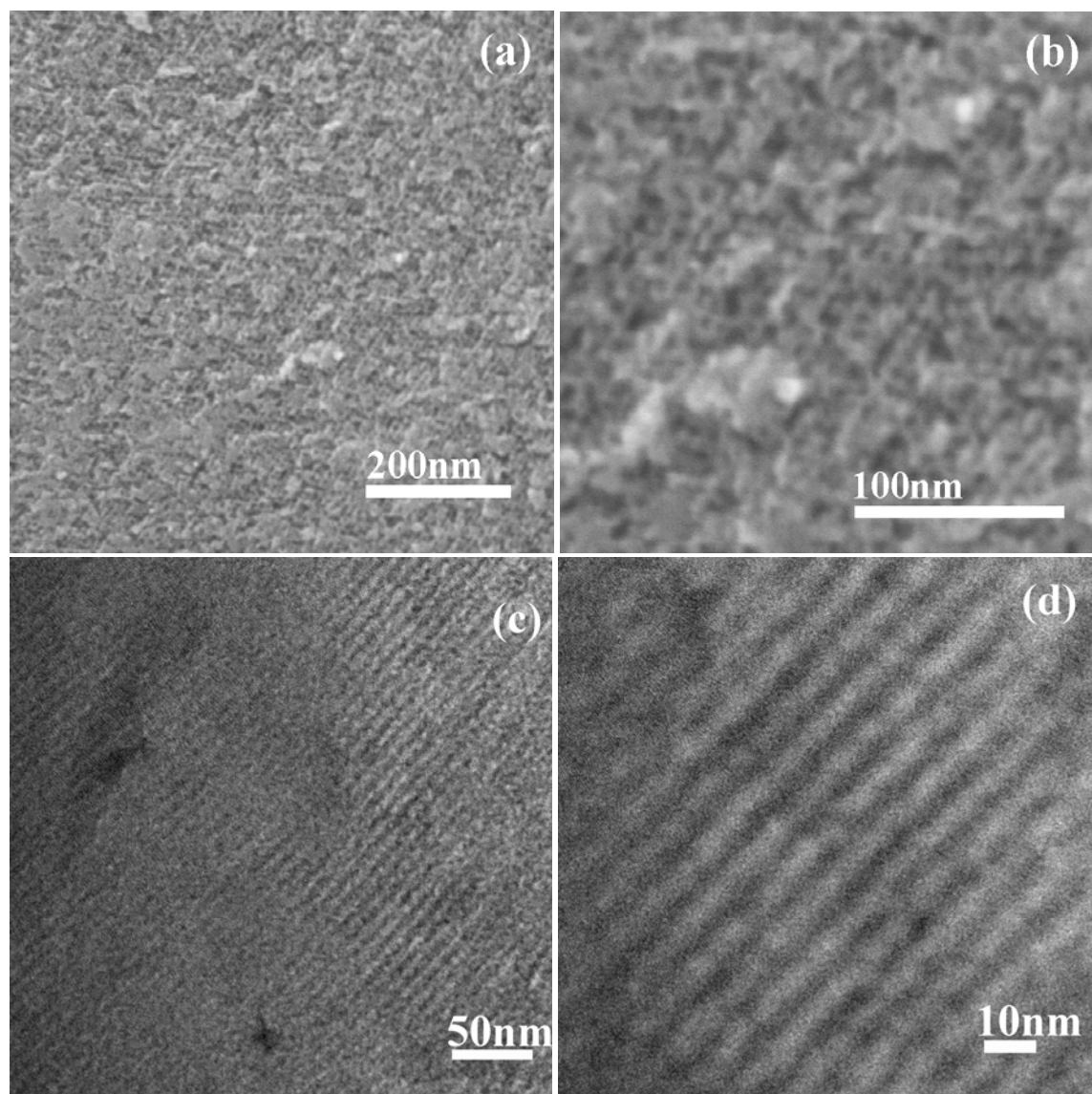


**Fig. 4** SEM (a and b) and TEM (c and d) images of OMC-F<sub>2.0</sub>.

### **3.4. Adsorption capacity evolution of OMCs and surface area effect on adsorptive removal of DEHP**

Adsorption behavior of the adsorbents depends on many aspects such as surface area, pore volume, pore diameter, size of guest adsorbate and surface chemical properties. Here we mainly personified the effect surface area of OMCs towards the adsorptive removal of DEHP model water pollutant. Equilibrium adsorption experiments were performed to determine the adsorption

capacity of the OMCs by the removal of DEHP water contaminate. **Fig. 5a** represents equilibrium adsorption curves of four different adsorbents for the removal of DEHP. It can be seen that adsorption capacity of OMC-F<sub>1.0</sub>, OMC-F<sub>2.0</sub>, OMC-F<sub>3.0</sub> and OMC-F<sub>4.0</sub> increased from 49 to 276, 364, 241 and 187 mg g<sup>-1</sup> respectively with increasing the equilibrium concentration of DEHP from 20 to 284 mg L<sup>-1</sup> and reached saturation progressively. This could be due to the increase in the driving force of the concentration gradient, as an increase in the initial DEHP concentration could accelerate the diffusion of DEHP into the porous channel of OMCs adsorbents.<sup>31</sup> As can be seen in **Fig. 5b** and **Table 2**, with the increasing of surface area of OMC-F<sub>1.0</sub> and OMC-F<sub>2.0</sub> from 1660 to 1801 m<sup>2</sup> g<sup>-1</sup>, the adsorption capacities were increased from 276 to 364 mg g<sup>-1</sup> respectively. Similarly, with the decrease in surface area of OMC-F<sub>3.0</sub> and OMC-F<sub>4.0</sub> from 1644 to 956 m<sup>2</sup> g<sup>-1</sup>, the adsorption capacities were decreased from 241 to 187 mg g<sup>-1</sup>. OMC-F<sub>2.0</sub> had the highest surface area (1801 m<sup>2</sup> g<sup>-1</sup>) and exhibited the highest adsorption capacity (364 mg g<sup>-1</sup>) amongst the all four OMCs. It suggests that adsorption capacity of OMCs for the removal of DEHP depended on surface area. Importantly, OMC-F<sub>1.0</sub> and OMC-F<sub>3.0</sub> do not have large surface area differences (1660 and 1644 m<sup>2</sup> g<sup>-1</sup> respectively) but adsorption capacity differences bit higher side (276 and 241 mg g<sup>-1</sup>) was noted. This could be due to the difference of micropore area and external surface area, as it presented in **Table 2**. Since the molecular size of DEHP is in nano range less than 2 nm, thus uniform micropore area can also welcome the DEHP molecule to occupy the place in internal area developed by micropores. However, micropore area difference of OMC-F<sub>1.0</sub> and OMC-F<sub>3.0</sub> was very high, 1101 and 684 m<sup>2</sup> g<sup>-1</sup> respectively, and it is not in correlation with adsorption capacity data. On the other hand, external surface area of OMC-F<sub>1.0</sub> and OMC-F<sub>3.0</sub> increased from 559 to 960 m<sup>2</sup> g<sup>-1</sup> respectively and it is also not correlation with adsorption capacity. As can be seen in **Table 2**, the large part of BET surface



area of OMC-F<sub>4.0</sub> is generated by mesopore volume and similar trends are noted in all other three OMCs. Therefore, adsorption capacity was mainly depend on the BET surface area of OMCs for the removal of DEHP water.

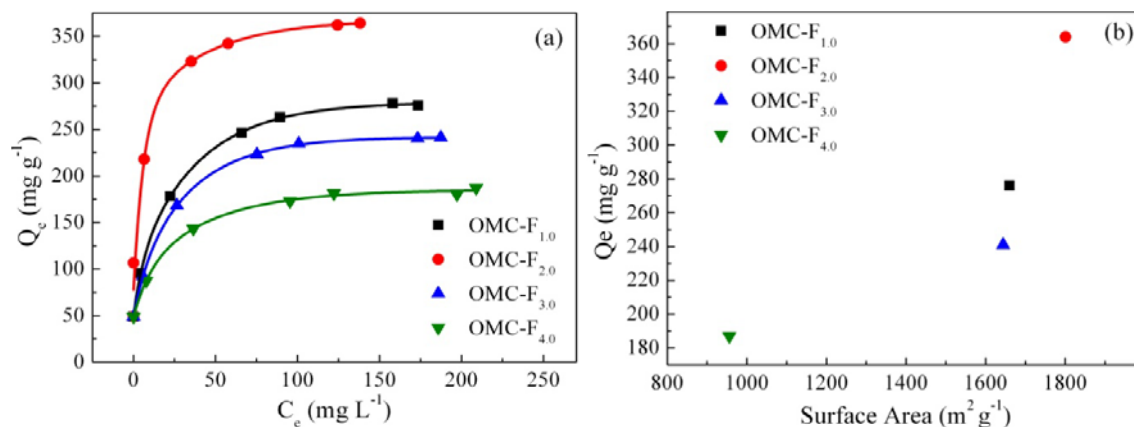


**Fig. 5** Adsorption capacity evaluation curve (a) of OMC-F<sub>1.0-4.0</sub> by varying the concentration gradient of model water pollutant DEHP and (b) is comparative plot of surface area vs adsorption capacity of OMC-F<sub>1.0-4.0</sub>.

### 3.5. Mathematical model fitting for decontamination of DEHP by OMCs

Obtained adsorption equilibrium data of OMCs from the decontamination of DEHP water pollutant were treated with two mathematical models Langmuir and Freundlich. Langmuir model assumes that adsorption occurs onto the homogeneous surfaces by monolayer coverage and no transmigration of the adsorbate in the plane of the surface.<sup>36</sup> Straight line equation is as follows:

$$\frac{C_e}{Q_e} = \frac{1}{Q_m K_L} + \frac{1}{Q_m} C_e \quad (2)$$

where  $C_e$  is the equilibrium concentration of the adsorbate (mg L<sup>-1</sup>),  $Q_e$  is the amount of adsorbate adsorbed per unit mass of adsorbent (mg g<sup>-1</sup>),  $K_L$  is Langmuir adsorption constant (L mg<sup>-1</sup>) and  $Q_m$  is the theoretical maximum adsorption capacity (mg g<sup>-1</sup>). The essential characteristics of Langmuir equation can be expressed in terms of a dimensionless separation factor  $R_L$ ,<sup>31</sup> which is defined as:

$$R_L = \frac{1}{1+K_L C_0} \quad (3)$$

where  $K_L$  is the Langmuir isotherm constant ( $L \text{ mg}^{-1}$ ) and  $C_0$  is the initial DEHP concentration ( $\text{mg L}^{-1}$ ). The  $R_L$  value indicates the type of isotherm to be either favorable ( $0 < R_L < 1$ ), unfavorable ( $R_L > 1$ ), linear ( $R_L = 1$ ) or irreversible ( $R_L = 0$ ).

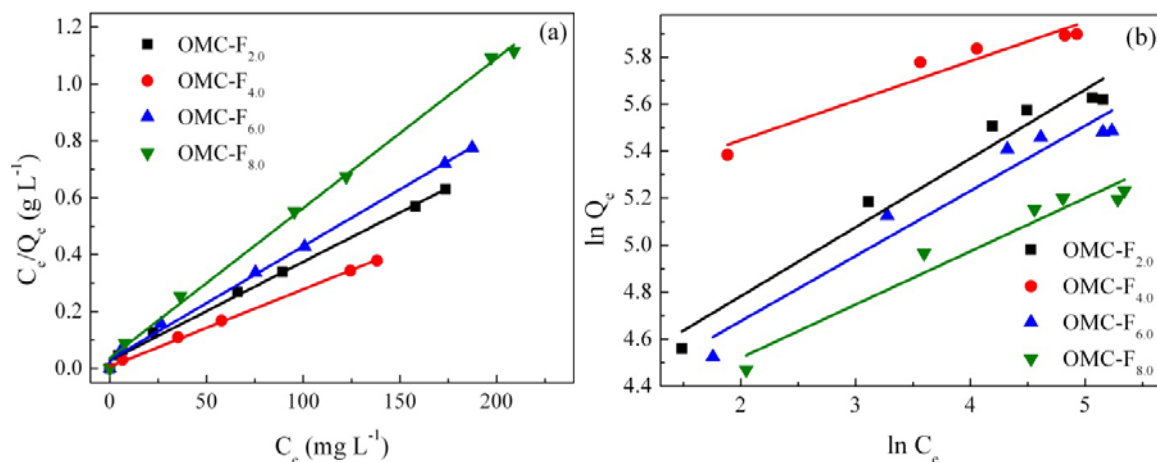


**Fig. 5** Mathematical model fitting of experimental data of adsorptive removal of DEHP by OMC-F<sub>1.0-4.0</sub>, Langmuir model (a) and Freundlich model (b).

Freundlich model assumes that it occurs at heterogeneous surface and can allow the guest object as multilayer manner. The logarithmic straight line equation is as follows:

$$\ln Q_e = \ln K_F + \frac{1}{n} \ln C_e \quad (4)$$

where  $K_F$  ( $L \text{ mg}^{-1}$ ) is the Freundlich constants and  $1/n$  is the heterogeneity factor.  $K_F$  is defined as an adsorption or distribution coefficient representing the amount of adsorbate adsorbed on an adsorbent for a unit equilibrium concentration while  $1/n$  giving an indication of how favorable the adsorption process. The  $1/n$  range between 0 and 1 is a measure of adsorption intensity or surface heterogeneity. If  $1/n$  value gets closer to zero, it becomes more heterogeneous. The  $1/n$

value below one indicates adsorption follow Langmuir model, while the value of  $1/n$  above to one indicates cooperative adsorption.<sup>37</sup>

**Table 3** Langmuir and Freundlich calculated parameters of DEHP adsorption on OMCs

Adsorbent	Langmuir				Freundlich		
	$Q_m$	$K_L$	$R_L$	$R^2$	$K_F$	$1/n$	$R^2$
OMC-F <sub>1,0</sub>	286	0.13	0.027-0.287	0.9962	55	0.3376	0.9755
OMC-F <sub>2,0</sub>	370	0.40	0.008-0.110	0.9987	83	0.3353	0.8521
OMC-F <sub>3,0</sub>	250	0.13	0.025-0.275	0.9973	53	0.3119	0.975
OMC-F <sub>4,0</sub>	189	0.14	0.023-0.260	0.9975	52	0.2537	0.9799

The experimental data for the removal of DEHP by OMCs were well fitted in Langmuir model (**Fig. 5a**). From the **Fig. 5b** it appears that the present adsorption process does not ideally follow Freundlich isotherm model and exhibits deviation from linearity over the entire concentration range. However, if the total concentration range is divided into several regions, good fits to the experimental data can be noted specially in the lower concentration range. Therefore, it concludes that the Freundlich equation cannot describe the adsorption process at higher concentration ranges for the removal of DEHP by OMCs. The parameters calculated from both model as above explained are presented in **Table 3**. Comparatively the correlation coefficient  $R^2$  of Langmuir model was better than Freundlich model, especially for OMC-F<sub>2,0</sub> of 0.9987 and 0.8521. It indicates that adsorption occurred in monolayer manner in high surface area OMCs. Moreover, calculated maximum monolayer adsorption capacity  $Q_m$  from Langmuir model of 370 mg g<sup>-1</sup> was near to experimental adsorption capacity of 364 mg g<sup>-1</sup>. It also indicates that adsorptive removal of DEHP by OMCs depended on the surface area trend. The dimensionless separation factor  $R_L$  of Langmuir model calculated from the equation (3) is

presented in **Table 3**. The obtained  $R_L$  values of all the OMCs for Langmuir model were between 0.008-0.287 which indicates adsorption in more favorable rather than irreversible. The  $1/n$  values calculated from Freundlich model of all OMCs were between 0.2537-0.3376 which is below the one and not very close to zero indicating high affinity to Langmuir adsorption. Therefore, it concludes that Langmuir model is thus found the better prediction for the adsorptive removal of DEHP in all concentration.

#### 4. Conclusion

We report the one-step assembly of tri-constituents via EISA method for the synthesis of high surface area OMCs. The organic precursor of phloroglucinol-formaldehyde was in-situ prepared in the one-step assembly of tri-constituents. The molar ratio variation of formaldehyde to phloroglucinol from 1.0 to 4.0 was able to tune the surface area of OMCs from 956 to 1801  $\text{m}^2 \text{g}^{-1}$ . Small angle XRD patterns and TEM images demonstrated that OMCs were highly ordered materials with hexagonal space symmetry of  $p6mm$  and SEM images revealed that OMC-F<sub>2.0</sub> was highly mesoporous material. The batch adsorption experimental studies for the decontamination of DEHP were evaluated by all four OMCs of different surface area and adsorption capacity revealed that decontamination of DEHP deepened on the surface area. The maximum adsorption capacity of 364  $\text{mg g}^{-1}$  was observed at highest surface area 1801  $\text{m}^2 \text{g}^{-1}$  of OMC-F<sub>2.0</sub>. The treatment of experimental data with two well know mathematical adsorption model Langmuir and Freundlich revealed that adsorption of DEHP occurred in monolayer manner and followed the Langmuir adsorption isotherms in the high surface area mesoporous ordered carbon. Therefore, it believe that adsorptive decontamination of DEHP water pollutant

depended on the surface area and mesoporosity and the OMCs derived by the one-step assembly method have great future prospect for the removal of various hazardous environmental pollutants.

### Acknowledgment

This work was financially supported by the National Natural Science Foundation of China (21207099, 21273162), the Science and Technology Commission of Shanghai Municipality, China (11nm0501000, 12ZR1451100), Key Subject of Shanghai Municipal Education Commission (J50102) and the Fundamental Research Funds for the Central Universities (2011KJ023). Pranav K. Tripathi acknowledges the Chinese Scholarship Council, Govt. of China and Ministry of Higher Education, Govt. of India for the research fellowship.

### REFERENCES

1. I. Ali, *Chem. Rev.*, 2012, **112**, 5073-5091.
2. P. Roslev, K. Vorkamp, J. Aarup, K. Frederiksen and P. H. Nielsen, *Water Res.*, 2007, **41**, 969-976.
3. E. Yuwatini, N. Hata and S. Taguchi, *J. Environ. Monit.*, 2006, **8**, 191-196.
4. International Agency for Research on Cancer, *Overall evaluations of carcinogenicity*, Lyon, 1987.
5. M. M. Abdel daiem, J. Rivera-Utrilla, R. Ocampo-Pérez, J. D. Méndez-Díaz and M. Sánchez-Polo, *J. Environ. Manage.*, 2012, **109**, 164-178.
6. L. Zhang, L. Dong, L. Ren, S. Shi, L. Zhou, T. Zhang and Y. Huang, *J. Environ. Sci.*, 2012, **24**, 335-342.
7. C. Dargnat, M. J. Teil, M. Chevreuil and M. Blanchard, *Sci. Total Environ.*, 2009, **407**, 1235-1244.
8. S. E. P. Agency, <http://apps.sepa.org.uk/spripa/Pages/SubstanceInformation.aspx?pid=32>.
9. P. K. Tripathi, L. Gan, M. Liu and N. N. Rao, *J. Nanosci. Nanotechnol.*, 2014, **14**, 1823-1837.
10. C. He and X. Hu, *Chem. Res.*, 2011, **50**, 14070-14083.
11. X. Zhuang, Y. Wan, C. Feng, Y. Shen and D. Zhao, *Chem. Mater.*, 2009, **21**, 706-716.
12. G. M. Walker and L. R. Weatherley, *Chem. Eng. J.*, 2001, **83**, 201-206.
13. P. K. Tripathi, M. Liu, L. Gan, J. Qian, Z. Xu, D. Zhu and N. N. Rao, *J. Mater. Sci.*, 2013, **48**, 8003-8013.

14. M. E. Davis, *Nature*, 2002, **417**, 813-821.
15. M. Teng, J. Qiao, F. Li and P. K. Bera, *Carbon*, 2012, **50**, 2877-2886.
16. R. Liu, Y. Shi, Y. Wan, Y. Meng, F. Zhang, D. Gu, Z. Chen, B. Tu and D. Zhao, *J. Am. Chem. Soc.*, 2006, **128**, 11652-11662.
17. Z. Li, X. Wang, C. Wang and L. Yin, *RSC Adv.*, 2013, **3**, 17097-17104.
18. W. Gao, Y. Wan, Y. Dou and D. Zhao, *Adv. Energy Mater.*, 2011, **1**, 115-123.
19. Y. Zhai, Y. Dou, X. Liu, S. S. Park, C.-S. Ha and D. Zhao, *Carbon*, 2011, **49**, 545-555.
20. Y. Huang, H. Cai, T. Yu, F. Zhang, F. Zhang, Y. Meng, D. Gu, Y. Wan, X. Sun, B. Tu and D. Zhao, *Angew. Chem. Int. Ed.*, 2007, **46**, 1089-1093.
21. J. Wang, C. Xue, Y. Lv, F. Zhang, B. Tu and D. Zhao, *Carbon*, 2011, **49**, 4580-4588.
22. K. Hou, A. Zhang, M. Liu and X. Guo, *RSC Adv.*, 2013, **3**, 25050-25057.
23. B. You, Z. Zhang, L. Zhang, J. Yang, X. Zhu and Q. Su, *RSC Adv.*, 2012, **2**, 5071-5074.
24. C. Liang and S. Dai, *J. Am. Chem. Soc.*, 2006, **128**, 5316-5317.
25. L. Liu, F. Y. Wang, G. S. Shao, T. Y. Ma and Z. Y. Yuan, *Carbon*, 2010, **48**, 2660-2664.
26. P. K. Tripathi, M. Liu, Y. Zhao, X. Ma, L. Gan, O. Noonan and C. Yu, *J. Mater. Chem. A*, 2014, DOI: 10.1039/c4ta00578c.
27. M. Bodzek, M. Dudziak and K. Luks-Betlej, *Desalination*, 2004, **162**, 121-128.
28. P. K. Tripathi, L. Gan, M. Liu, X. Ma, Y. Zhao, D. Zhu, Z. Xu, L. Chen and N. N. Rao, *Mater. Lett.*, 2014, **120**, 108-110.
29. L. Bromberg and E. Magner, *Langmuir*, 1999, **15**, 6792-6798.
30. K. S. W. Sing, D. H. Everett, R. A. W. Haul, L. Moscou, R. A. Pierotti, J. Rouquerol and T. Siemieniewska, *Pure Appl. Chem.*, 1985, **57**, 603-619.
31. N. Mohammadi, H. Khani, V. K. Gupta, E. Amereh and S. Agarwal, *J. Colloid Interface Sci.*, 2011, **362**, 457-462.
32. A. Gil, *Adsorption*, 1998, **4**, 197-206.
33. A. P. Katsoulidis and M. G. Kanatzidis, *Chem. Mater.*, 2011, **23**, 1818-1824.
34. C. C. Ting, Y. C. Pan, S. Vetrivel, D. Saikia and H. M. Kao, *RSC Adv.*, 2012, **2**, 2221-2224.
35. D. D. Zhou, Y. J. Du, Y. F. Song, Y. G. Wang, C. X. Wang and Y. Y. Xia, *J. Mater. Chem. A*, 2013, **1**, 1192-1200.
36. I. Langmuir, *J. Am. Chem. Soc.*, 1916, **38**, 2221-2295.
37. K. Fytianos, E. Voudrias and E. Kokkalis, *Chemosphere*, 2000, **40**, 3-6.